Valence-band mixing effects on hole oscillations in coupled quantum wells

C. Juang
Division T200, Optoelectronics and Systems Laboratories, ITRI, Hsinchu, Taiwan 310, Republic of China

P. A. Chen and C. Y. Chang
Institute of Electronics, National Chiao Tung University, Hsinchu, Taiwan 300, Republic of China
(Received 17 September 1992)

Valence-band mixing effects on the dynamics of the heavy- and light-hole oscillations in coupled quantum wells are described by a numerical implementation using the time-dependent Schrödinger equation with the Luttinger Hamiltonian. With a nonzero in-plane wave vector ($k_{\parallel} \neq 0$), mixing tunneling (between heavy- and light-hole states) and spatial tunneling (from one well to the other) occur at the same time. This time-dependent analysis clearly resolves these two tunneling mechanisms and shows several effects which have not been addressed by previous time-independent analysis.

I. INTRODUCTION

Recently, there has been considerable interest in the investigation of the tunneling effects in the coupled quantum-well structures that consist of two quantum wells located sufficiently close together.[1-12] Electron spatial oscillations via coherent tunneling through a classically impenetrable thin barrier in a very short period of time have bee reported.[1] The emission of an electromagnetic wave due to this spatial oscillation has been observed.[2] In addition, the application of the time-development operator according to the time-dependent Schrödinger equation has been used to describe the oscillation frequency and oscillation amplitude associated with these tunneling mechanisms.[3,4]

In the case of the hole tunneling in the coupled quantum wells, the tunneling mechanisms are significantly complicated due to band-mixing effects.[5-12] Two possible mechanisms, spatial tunneling (from one well to the other) and mixing tunneling (between heavy- and light-hole states), are involved in the process. An illustration is given in Fig. 1. Leo *et al.*, have shown that heavy- to light-hole mixing tunneling is less effective compared with heavy-hole spatial tunneling.[5] However, some theoretical studies have suggested the importance of band-mixing effect in the hole tunneling in coupled wells and double barrier structures.[6-8] It is pointed out that heavy-hole tunneling can be much faster due to band mixing effects. Although no conclusive evidence is reported, several experiments also point out the significance of band-mixing effects on the spatial tunneling of the heavy hole in coupled quantum wells.[9-11] In addition, the importance of band-mixing effects can be greatly enhanced if the mixing is further induced by an external stress.[12]

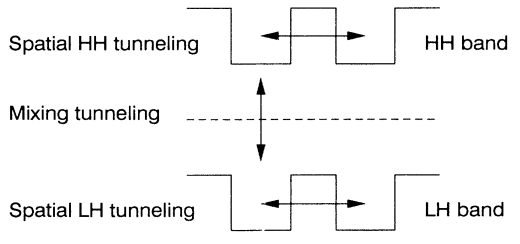

FIG. 1. Schematic potential profiles of mixing tunneling, spatial heavy-hole tunneling, and spatial light-hole tunneling in light- and heavy-hole bands of coupled quantum wells with band-mixing effects.

In previous theoretical works,[6-8,12] the Luttinger Hamiltonian is incorporated into the time-independent Schrödinger equation to obtain a description of mixing effects. This work goes beyond the time-independent analysis by using the time-dependent Schrödinger equation with the Luttinger Hamiltonian. In this approach, valence-band mixing is taken into consideration by the Luttinger Hamiltonian, and the evolution of the heavy- and light-hole wave functions is shown by the time-dependent Schrödinger operator with the Luttinger Hamiltonian. Using this time-dependent analysis, the mixing tunneling and spatial tunneling, which happen at the same time, can be clearly resolved. This is not possible by previous time-independent analysis.[6-18,12] In addition, using a properly defined tunneling probability, some properties based on this time-dependent analysis can be shown. For example, light- to heavy-hole mixing tunneling is found to be more effective than heavy- to light-hole mixing tunneling, and induces a significant spatial heavy-hole tunneling. The mixing tunneling, which has a higher oscillation frequency, also modulates the spatial tunneling. For the spatial tunneling, band-mixing effects seem to slow down rather than speed up the tunneling process for both pure heavy- and light-hole wave functions.

Section II summarizes the numerical techniques for solving the time-dependent Schrödinger equations with the Luttinger Hamiltonian. For $k_{\parallel}=0$ (no mixing), the spatial heavy- and light-hole tunneling are described in Sec. III. Section IV shows mixing tunneling, spatial heavy-hole tunneling, and spatial light-hole tunneling for $k_{\parallel} \neq 0$ (band mixing). The tunneling probability, oscillation frequency, and oscillation amplitude are also calculated.

II. METHOD OF NUMERICAL ANALYSIS

The valence band can be described by a 4×4 Luttinger-Kohn Hamiltonian with bias elements $|3/2,\pm 3/2\rangle$ as heavy-hole states and $|1/2,\pm 1/2\rangle$ as light-hole states. To further simplify the calculations, the 4×4 Luttinger-Kohn Hamiltonian is converted to a block diagonal matrix using a unitary transformation as described in detail in Refs. 13 and 14.

$$H_h=\begin{bmatrix} P+Q+V_h(z) & \tilde{R} & 0 & 0 \\ \tilde{R}^* & P-Q+V_h(z) & 0 & 0 \\ 0 & 0 & P-Q+V_h(z) & \tilde{R} \\ 0 & 0 & \tilde{R}^* & P+Q+V_h(z) \end{bmatrix} = \begin{bmatrix} H_h^u & 0 \\ 0 & H_h^l \end{bmatrix}, \tag{1}$$

where

$$P=\frac{1}{2}\left[\frac{\hbar^2}{m_0}\right]\gamma_1 k_{\parallel}^2-\frac{1}{2}\left[\frac{\hbar^2}{m_0}\right]\frac{\partial}{\partial z}\gamma_1\frac{\partial}{\partial z},$$

$$Q=\frac{1}{2}\left[\frac{\hbar^2}{m_0}\right]\gamma_2 k_{\parallel}^2+\left[\frac{\hbar^2}{m_0}\right]\frac{\partial}{\partial z}\gamma_2\frac{\partial}{\partial z},$$

$$\tilde{R}=\left[\frac{\hbar^2}{m_0}\right]\left[\frac{\sqrt{3}}{4}(\gamma_2+\gamma_3)k_{\parallel}^2-\frac{\sqrt{3}}{2}k_{\parallel}\left[\gamma_3\frac{\partial}{\partial z}+\partial\partial z\gamma_3\right]\right], \tag{2}$$

and H_h^u and H_h^l are the upper and lower blocks of the Hamiltonian, $V_h(z)$ is the quantum-well potential for the hole, $\gamma_1,\gamma_2,\gamma_3$ are the Luttinger parameters and are position dependent in the heterojunction structures, m_0 is the electron rest mass, $k_{\parallel}^2=k_x^2+k_y^2$. The symmetry coupled quantum wells are grown along the [001] direction, and denoted as the z axis. Note that the momentum operators in P, Q, $\tilde{R}$ are modified to the form of BenDaniel and Duke's effective Hamiltonian[15,16] so as to preserve the conservation of the probability.[17] The new basis elements become a linear combination of the heavy-hole and light-hole states[13,14]

$$\begin{aligned} |1\rangle&=\alpha|3/2,3/2\rangle-\alpha^*|3/2,-3/2\rangle, \\ |2\rangle&=\beta|3/2,-1/2\rangle-\beta^*|3/2,1/2\rangle, \\ |3\rangle&=\beta|3/2,-1/2\rangle+\beta^*|3/2,1/2\rangle, \\ |4\rangle&=\alpha|3/2,3/2\rangle+\alpha^*|3/2,-3/2\rangle, \end{aligned} \tag{3}$$

where β and α are constant complex numbers. Since H_h^u (corresponding to $|1\rangle$ and $|2\rangle$ state) are decoupled from H_h^l (corresponding to $|3\rangle$ and $|4\rangle$ states), they can be treated separately. Assuming that $|1\rangle$ and $|2\rangle$ states are heavy-hole (HH1) and light-hole states (LH1), respectively, the time-dependent Schrödinger equation with the upper block of the Luttinger-Kohn Hamiltonian can be written by

$$H_h^u\begin{bmatrix}\phi^1(x,t)\\ \phi^2(x,t)\end{bmatrix}=ih\frac{\partial}{\partial t}\begin{bmatrix}\phi^1(x,t)\\ \phi^2(x,t)\end{bmatrix}, \tag{4}$$

where $\phi^1(x,t)$ and $\phi^2(x,t)$ are HH1 and LH1 state envelope wave functions, respectively. The discretization of Eq. (4) with respect to time gives[17]

$$\left[1+\frac{i\delta}{2\hbar}H_h^u\right]\begin{bmatrix}\phi_{n+1}^1\\ \phi_{n+1}^2\end{bmatrix}=\left[1-\frac{i\delta}{2\hbar}H_h^u\right]\begin{bmatrix}\phi_n^1\\ \phi_n^2\end{bmatrix}, \tag{5}$$

where δ and n are the time spacing and time index, respectively. In addition, H_h^u can be converted to a difference matrix operator with respect to space and is given by

$$H_h^u\begin{bmatrix}\phi_{j,n}^1\\ \phi_{j,n}^2\end{bmatrix}=\begin{bmatrix}A_{j-1} & A_j & A_{j+1} & B_{j-1} & B_j & B_{j+1}\\ C_{j-1} & C_j & C_{j+1} & D_{j-1} & D_j & D_{j+1}\end{bmatrix}\begin{bmatrix}\phi_{j-1,n}^1\\ \phi_{j,n}^1\\ \phi_{j+1,n}^1\\ \phi_{j-1,n}^2\\ \phi_{j,n}^2\\ \phi_{j+1,n}^2\end{bmatrix}, \tag{6}$$

where

$$
\begin{aligned}
A_j &= \left[\frac{\hbar^2}{2m_0}\right](\gamma_{1j}+\gamma_{2j})k_\parallel^2+\left[\frac{\hbar^2}{m_0\epsilon^2}\right]\left[\frac{1}{m_{j+1}^{*1}+m_j^{*1}}+\frac{1}{m_{j-1}^{*1}+m_j^{*1}}\right]+V_{hj}\ ,\\
A_{j-1} &= -\left[\frac{\hbar^2}{m_0\epsilon^2}\right]\frac{1}{m_{j-1}^{*1}+m_j^{*1}},\quad A_{j+1}=-\left[\frac{\hbar^2}{m_0\epsilon^2}\right]\frac{1}{m_{j+1}^{*1}+m_j^{*1}}\ ,\\
B_j &= \left[\frac{\hbar^2}{m_0}\right]\left[\frac{\sqrt{3}}{4}(\gamma_{2j}+\gamma_{3j})k_\parallel^2+\frac{\sqrt{3}\gamma_{3j}k_\parallel}{\epsilon}\right],\\
B_{j-1} &= 0,\quad B_{j+1}=-\left[\frac{\hbar^2}{m_0}\right]\frac{\sqrt{3}(\gamma_{3j}+\gamma_{3j+1})k_\parallel}{2\epsilon}\ ,\\
C_j &= \left[\frac{\hbar^2}{m_0}\right]\left[\frac{\sqrt{3}}{4}(\gamma_{2j}+\gamma_{3j})k_\parallel^2+\frac{\sqrt{3}\gamma_{3j}k_\parallel}{\epsilon}\right],\\
C_{j-1} &= -\left[\frac{\hbar^2}{m_0}\right]\frac{\sqrt{3}(\gamma_{3j}+\gamma_{3j-1})k_\parallel}{2\epsilon},\quad C_{j+1}=0\ ,\\
D_j &= \left[\frac{\hbar^2}{2m_0}\right](\gamma_{1j}-\gamma_{2j})k_\parallel^2+\left[\frac{\hbar^2}{m_0\epsilon^2}\right]\left[\frac{1}{m_{j+1}^{*2}+m_j^{*2}}+\frac{1}{m_{j-1}^{*2}+m_j^{*2}}\right]+V_{hj}\ ,\\
D_{j-1} &= -\left[\frac{\hbar^2}{m_0\epsilon^2}\right]\frac{1}{m_{j-1}^{*2}+m_j^{*2}},\quad D_{j+1}=-\left[\frac{\hbar^2}{m_0\epsilon^2}\right]\frac{1}{m_{j+1}^{*2}+m_j^{*2}}\ ,\\
m_j^{*1} &= \frac{1}{\gamma_{1j}-2\gamma_{2j}},\quad m_j^{*2}=\frac{1}{\gamma_{1j}+2\gamma_{2j}}\ .
\end{aligned}
\tag{7}
$$

Note that the first-order differential terms in operators $\tilde{R}$ and $\tilde{R}^*$ are discretized using the front and back differencing techniques, respectively, to ensure Hermiticity of the upper block matrix H_h^u. By inserting Eq. (6) into Eq. (5), the resulting difference equation can be obtained. This difference equation can be written in linear $Ax=b$ matrix equation with A being a complex symmetry matrix. By calling the IMSL subroutine on a supercomputer, this linear matrix equation is solved. With an initial wave function, time evolution can be obtained by iterative multiplications of the inveted matrix. In the numerical calculations, the space interval ϵ and time interval δ are chosen to be 1 Å and 4 fsec (10^{-15}).

III. WITHOUT MIXING ($k_\parallel=0$)

Coupled quantum-well systems of 25-15-25 (first well width–barrier width–second well width in angstroms) with a barrier height of 0.2506 eV, which corresponds to 50 at% Al content in an $Al_xGa_{1-x}As/GaAs$ system with a 60 to 40 ratio of ΔE_c to ΔE_v are investigated. The Luttinger parameters $(\gamma_1,\gamma_2,\gamma_3)$ are chosen to be 6.85, 2.1, 2.9 in the well region and 5.15, 1.39, 2.10, which are obtained by a linear interpolation of the Luttinger parameters of GaAs and AlAs, in the barrier region.[18] The initial wave functions are the heavy- and light-hole wave functions in the first well, and the tunneling process is initiated at $t=0$.

Figure 2 shows the interwell tunneling of the heavy hole and light hole in the 25-15-25 Å quantum wells. The initial wave function is the eigenfunction of the first well. In Fig. 2, the heavy-hole wave packet tunnels from the first well to the second well during around the first 252 fsec. However, as time increases, the wave packet tunnels back to the first well. As shown, a larger portion of the wave packet is involved in this tunneling process. The arrows in the figures indicate the oscillation of the wave packet. Since there is no mixing ($k_\parallel=0$), the only factor that differentiates the tunneling processes of the heavy and light holes is the effective mass. The lighter the particle is, the faster the tunneling process should be. Thus, it takes a much shorter time for the light-hole wave packet to reach the peak in the second well and then to tunnel back.

In order to further characterize the properties of interwell tunneling based on time-dependent analysis, the tunneling probabiity $P(t)$ is defined as

$$P(t)=|\langle\phi_2^i(x,0)|\phi_1^i(x,t)\rangle|^2\ , \tag{8}$$

where $\phi_2^i(x,0)$, $i=1,2$, denotes the heavy-hole or light-hole eigenfunctions in the second well, and $\phi_1^i(x,t)$ denotes the heavy-hole or light-hole wave functions in the first well. In the beginning the wave packet is mainly located in the first well, and $P(t)$ is small. When the wave packet has left the first well and tunnels into the second well, the $P(t)$ approaches 1. Figure 3 shows the tunneling probability $P(t)$ for the heavy- and light-hole wave

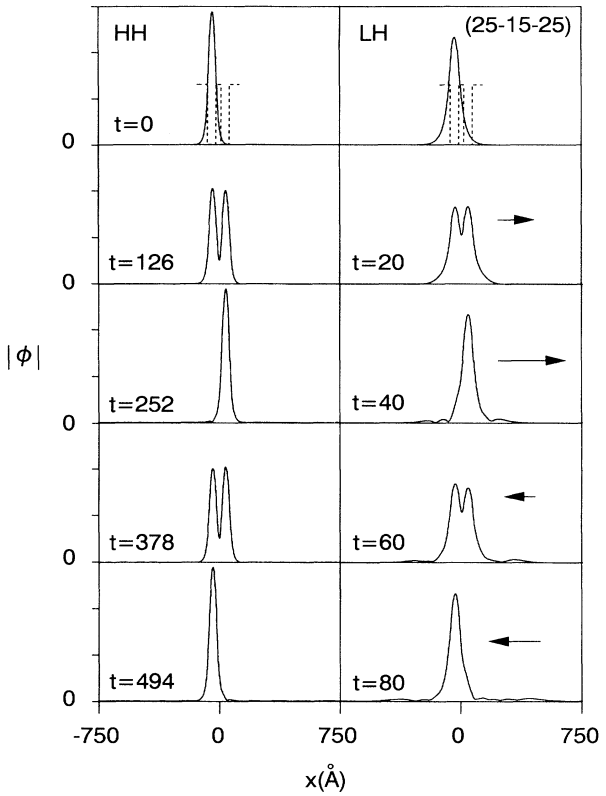

FIG. 2. An interwell tunneling of the heavy hole and the light hole in 25-15-25 Å coupled quantum wells without band mixing ($k_{\|}=0$). The position of the coupled quantum wells is shown by the dotted line at the $T=0$ frame. The arrows indicate the oscillation of the wave packet.

packets. From Fig. 3, the oscillation frequency can be defined as the inverse of a tunneling cycle T, which is the time required for the tunneling probability $P(t)$ to reach from one local maximum to the next local maximum. The peak-to-valley ratio, which characterizes the amplitude of the oscillation, is the ratio of a local maximum to a local minimum of the tunneling probability $P(t)$.

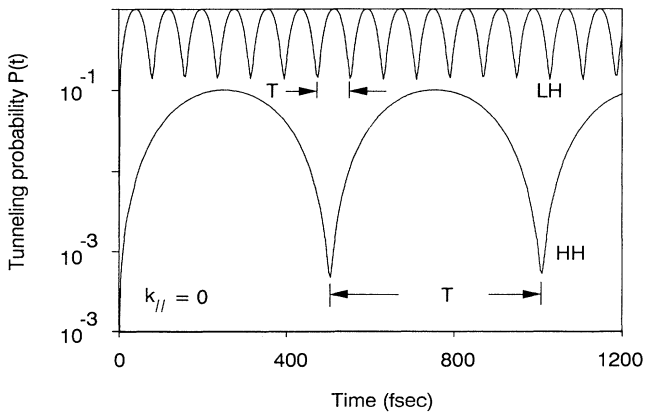

FIG. 3. Tunneling probability defined in Eq. (8) for heavy- and light-hole wave packets in 25-15-25 Å coupled quantum wells without band mixing ($k_{\|}=0$).

The oscillation frequency and amplitude are then compared. As shown, the oscillation frequency of the heavy hole is smaller than that of the light hole (1.98 to 12.5 THz) since the effective mass of the heavy hole is large. In addition, there is also a significant difference in the peak-to-valley ratio. The typical peak-to-valley ratios for the heavy and light holes are 213 and 5.61. A heavier particle also gives a larger peak-to-valley ratio.

IV. WITH BAND MIXING ($k_{\|}\neq 0$)

The effects of valence-band mixing are studied using the same parameters, except that $k_{\|}$ is chosen to be 0.025 ($2\pi/a$), where a is the lattice constant of GaAs. With this nonzero in-plane wave vector $k_{\|}$, heavy- and light-hole wave functions are mixed together as the tunneling process goes on. So, spatial light-hole tunneling is possible when a pure heavy-hole wave packet is used as the initial function, and *vice versa*. Table I lists the coherent oscillation frequencies with and without band mixing of tunneling, spatial heavy-hole tunneling, and spatial light-hole tunneling. These results will be further discussed in this section.

A. Mixing tunneling

Mixing tunneling occurs between heavy- and light-hole states due to band-mixing effects, which have no comparison in the conduction band. In order to characterize the properties of the mixing tunneling based on the time-dependent analysis, one can define a probability factor $F(t)$ as the probability of finding the heavy hole in the heavy-hole band,

$$F(t)=\int_{\mathrm{HH}}\phi^{1}(x,t)\phi^{1*}(x,t)dx \ , \tag{9}$$

where $\phi^{1}(x,t)$ is the heavy-hole wave function. When $F(t)$ approaches 1, the wave packet is mainly located in the heavy-hole band. When $F(t)$ is small, the wave packet has left the heavy-hole band and tunnels into the light-hole band. Therefore, the oscillation frequency and amplitude of the mixing tunneling can be fully described by this probability factor $F(t)$.

Figure 4 shows $F(t)$ as a function of time for the heavy hole and the light hole. For a pure heavy hole (no probability at light-hole band), F is equal to 1 at the beginning. As time passes, it is shown that the wave packet oscillates between the heavy-hole band and the light-hole band with a high oscillation frequency (15.5 THz) and a small oscillation amplitude (peak-to-valley ratio 1.2). This indi-

TABLE I. Comparison of the coherent oscillation frequency f_c in THz (10^{12}) with and without band mixing of mixing tunneling, spatial heavy-hole tunneling, and spatial light-hole tunneling in 25-15-25 Å coupled quantum wells.

f_c	No mixing		Mixing	
(THz)	Spatial tunneling	Mixing	Spatial HH	Spatial LH
HH	1.98	15.5	0.86	15.4
LH	12.5	9.45	10.3	7.03

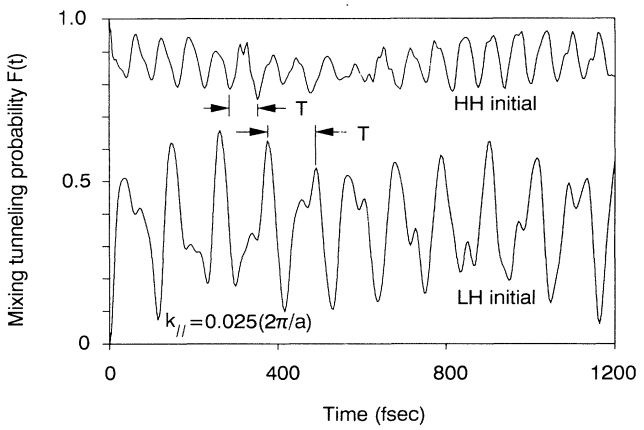

FIG. 4. Mixing tunneling probability factor $F(t)$ defined by Eq. (9) as a function of time for the heavy hole (HH initial) and light hole (LH initial) as initial wave packets in 25-15-25 Å coupled quantum wells with band mixing [$k_{\|}=0.025\ (2\pi/a)$].

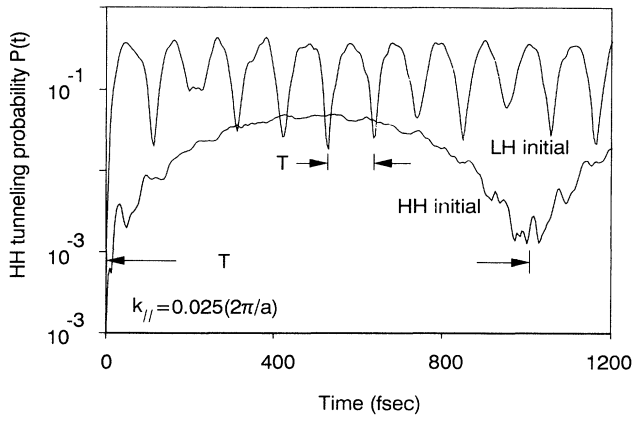

FIG. 5. Spatial tunneling probability of the heavy hole as a function of time using the heavy hole (HH initial) and light hole (LH initial) as initial wave packets in 25-15-25 Å coupled quantum wells with band mixing [$k_{\|}=0.025\ (2\pi/a)$].

cates that it takes a short time to tunnel between heavy- and light-hole states, and only a small portion of the wave packet is involved in the tunneling process (less than 25% wave packet found in the light-hole band at maximum). For a pure light hole, the tunneling cycle is longer (9.45THz) and the amplitude is larger (peak-to-valley ratio 4.3), meaning that a larger portion of the wave packet is involved in the tunneling process (more than 65% wave packet found in the heavy-hole band at maximum). This suggests that the light hole to heavy hole is more effective in the mixing tunneling.

B. Spatial heavy-hole tunneling

Spatial tunneling occurs between the first and the second wells in both the heavy hole band and the light hole band. In the absence of band-mixing effects ($k_{\|}=0$), spatial tunneling is similar to that in the conduction band, as described in Sec. III. However, by taking band-mixing effects into consideration, the tunneling process is significantly affected by band-mixing effects.

Using the same definition of the tunneling proability [Eq. (8)], Fig. 5 shows $P(t)$ of the heavy-hole wave function, which describes the spatial heavy-hole tunneling. For a pure initial heavy hole (HH), the heavy-hole wave packet undergoes spatial tunneling and mixing tunneling (from the heavy-hole to the light-hole band) at the same time. However, as discussed in Sec. IV A, the heavy- to light-hole tunneling is less effective in the mixing tunneling. Thus, the spatial tunneling is dominant, and the ripples in the $P(t)$ result from the modulation of the mixing tunneling. One other interesting result is that the oscillation frequency is smaller rather than larger than that of spatial heavy-hole tunneling when $k_{\|}=0$. [1.98 THz for $k_{\|}=0$ and 0.86 THz for $k_{\|}=0.025\ (2\pi/a)$]. This indicates that band-mixing effects slow down the tunneling process if a pure initial heavy-hole wave packet is used. The oscillation amplitude is also reduced more than five times when band-mixing effects are considered (peak-to-valley ratio 39). For a pure initial light hole, there is no wave packet in the heavy-hole band in the beginning. Due to the mixing tunneling, the particle tunnels into the heavy-hole band and proceeds to the spatial tunneling. As discussed in Sec. IV A, the light-hole to heavy-hole mixing tunneling is very effective. Thus a noticeable heavy-hole spatial tunneling occurs even though there is no wave packet in the heavy-hole band before tunneling. The oscillation frequency is 10.3 THz, and the peak-to-valley ratio is about 15.

C. Spatial light-hole tunneling

Figure 6 shows the tunneling probability [Eq. (8)] of the light-hole wave function, which describes the spatial light-hole tunneling. For a pure initial light hole (LH), spatial tunneling and mixing tunneling take place (from

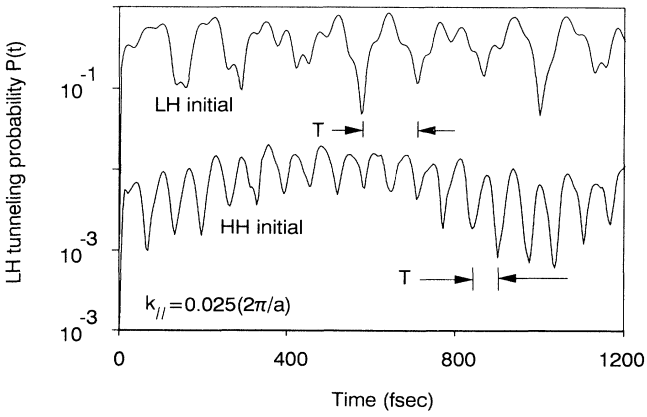

FIG. 6. Spatial tunneling probability of the light hole as a function of time using the heavy hole (HH initial) and light hole (LH initial) as initial wave packets in 25-15-25 Å coupled quantum wells with band mixing [$k_{\|}=0.025\ (2\pi/a)$].

the light-hole to the heavy-hole band) at the same time. Since mixing tunneling is effective, the spatial tunneling (7.03 THz) is less dominant and is significantly modulated by the mixing tunneling, which has a high oscillation frequency (9.45 THz). When compared with the spatial light-hole tunneling without mixing ($k_{\|}=0$), the oscillation frequency of the spatial light-hole tunneling with mixing becomes smaller. This also indicates that band-mixing effects slow down the light-hole tunneling process if a pure initial light-hole wave packet is used, which is consistent with the spatial tunneling of the heavy hole. For a pure initial heavy hole, there is no wave packet in the light-hole band in the beginning. Due to the mixing tunneling, the particle tunnels into the heavy-hole band and proceeds to the spatial tunneling. However, the heavy- to light-hole mixing tunneling is less effective. Thus, the light-hole spatial tunneling is less significant when a pure heavy hole is used as the initial wave function.

V. CONCLUSIONS

Compared to the time-independent analysis currently in use, the method presented in this work offers a better picture to describe the mixing tunneling and spatial heavy- and light-hole tunneling in coupled quantum wells. Time evolution of the heavy- and light-hole wave packets in the coupled quantum wells with and without band-mixing effects is shown by a numerical implementation of the time-development operator of the Schrödinger equation with the Luttinger Hamiltonian. With this time-dependent analysis light- to the heavy-hole mixing tunneling is found to be more effective than heavy- to light-hole mixing tunneling, and induces a significant spatial heavy-hole tunneling. The mixing tunneling, which has a higher oscillation frequency, also modulates the spatial tunneling. In addition, the band-mixing effects seem to slow down the spatial tunneling process for both pure heavy- and light-hole wave functions.

ACKNOWLEDGMENTS

This work in ITRI was supported by the Ministry of Economic Affairs the Republic of China under Project No. 38N1200, and the work in NCTU was supported by the National Science Council of the Republic of China under Contract No. NSC 81-0417-E-009-12.

[1]K. Leo, J. Shah, O Göbel, T. C. Damen, S. Schmitt-Rink, and W. Schäfer, Phys. Rev. Lett. **66**, 201 (1991).
[2]H. G. Roskos, M. C. Nuss, J. Shah, K. Leo, D. A. B. Miller, A. M. Fox, and K. Köhler, Phys. Rev. Lett. **68**, 2216 (1992).
[3]C. Juang, Phys. Rev. B **44**, 10 706 (1991).
[4]C. Juang and J. H. Chang, IEEE J. Quantum Electron. **28**, 2039 (1992).
[5]K. Leo, J. Shah, J. P. Gordon, T. C. Damen, D. A. B. Miller, C. W. Tu, and J. E. Cunningham, Phys. Rev. B **42**, 7065 (1990).
[6]R. Ferreira and G. Bastard, Europhys. Lett. **10**, 279 (1989).
[7]D. Z. Y. Ting, E. T. Yu, and T. C. McGill, Phys. Rev. B **45**, 3576 (1992).
[8]J. B. Xia, Phys. Rev. B **38**, 8365 (1988).
[9]T. B. Norris, N. Vodjdani, B. Vinter, E. Costard, and E. Böckenhoff, Phys. Rev. B **43**, 1867 (1991).
[10]M. Nido, M. G. W. Alexander, W. W. Rühle, and K. Köhler, Phys. Rev. B **43**, 1839 (1991).
[11]Ph. Roussignol, A. Vinattieri, L. Arraresi, M. Colocci, and A. Fasolino, Phys. Rev. B **44**, 8873 (1991).
[12]P. Lefebvre, and P. Bonnel, B. Gil, and H. Mathieu, Phys. Rev. B **44**, 5635 (1991).
[13]D. Ahn, S. L. Chuang, and Y. C. Chang, J. Appl. Phys. **64**, 4056 (1988).
[14]S. L. Chuang, Phys. Rev. B **43**, 9649 (1991).
[15]D. J. BenDaniel and C. B. Duke, Phys. Rev. **152**, 683 (1966).
[16]A. T. Meny, Superlatt. Microstruct. **11**, 31 (1992).
[17]C. Juang, K. J. Kuhn, and R. B. Darling, Phys. Rev. B **41**, 12 047 (1990).
[18]M. Altarelli, U. Ekenberg, and A. Fasolino, Phys. Rev. B **32**, 5138 (1985).